

# Low-Energy $\Lambda$ - $d$ Scattering and the Hypertriton with Separable Potentials\*†

J. H. HETHERINGTON§ AND L. H. SCHICK‡

*School of Physics, University of Minnesota, Minneapolis, Minnesota*

(Received 19 April 1965)

The  $\Lambda$ - $d$  scattering and  ${}_{\Lambda}H^3$  binding-energy problems are solved exactly using nonlocal separable  $S$ -wave potentials and a multiple-scattering formalism of the Faddeev type.  $\Lambda$ - $d$  scattering cross sections are presented for laboratory momenta in the range 100–250 MeV/ $c$ . No strong dependence of the  $\Lambda$ - $d$  scattering cross sections upon the low-energy  $\Lambda$ - $N$  scattering parameters is found. It is shown that the  $\Lambda$ - $N$  scattering data and the  ${}_{\Lambda}H^3$  binding energy cannot both be adequately fitted with purely attractive two-body potentials of the form used. Results are presented which illustrate the energy dependence of the  $S$  matrix and the nonconvergence of the multiple-scattering series for the low-energy scattering amplitude when a three-body bound state is present.

## I. INTRODUCTION

THIS is the third in a series of papers on the interaction at low energy of particles other than nucleons with deuterons. In this series a multiple-scattering formalism of the Faddeev<sup>1</sup> type is used to analyze the three-body problem under discussion. The individual two-body interactions for a given spin (and/or isospin) state are taken to be nonlocal separable (NLS)  $S$ -wave potentials.<sup>2</sup> With these potentials the three-body problem is solved exactly.<sup>3</sup>

The two previous works in this series dealt with  $K^-$ - $d$  and  $K^+$ - $d$  elastic scattering, respectively.<sup>4,5</sup> In the former the two-body particle-nucleon amplitudes were large and absorptive. In the latter these amplitudes were small and nonabsorptive. The low-energy  $S$ -wave  $\Lambda$ - $N$  amplitudes are large and nonabsorptive.<sup>6</sup> The  $\Lambda$ - $d$  problem is of interest as an extension of the previously developed formalism to a range of two-particle amplitudes complementary to those used before.

Physically the  $\Lambda$ - $d$  problem is a much cleaner application of our model than the kaon problems in that the Coulomb, mass-difference, and relativistic effects which had to be neglected in the kaon problems are absent here. Moreover, the  $\Lambda$ - $N$  scattering lengths and effective ranges are better known than the corresponding  $\bar{K}$ - $N$  and  $K$ - $N$  parameters.<sup>7</sup> Still, there are rather wide limits

on the numerical values of these low-energy  $\Lambda$ - $N$  parameters. Information from  $\Lambda$ - $d$  scattering might serve to narrow these limits.<sup>8</sup> Furthermore, the existence of a three-body bound state ( ${}_{\Lambda}H^3$ ) of known binding energy which may be investigated along with the scattering problem is an important feature that the kaon problems lacked.

Almost all previous treatments of  ${}_{\Lambda}H^3$  by other authors have been straightforward variational calculations,<sup>9</sup> the best of which are rather lengthy. Some of these calculations used  $\Lambda$ - $N$  potentials with hard cores,<sup>6,9,10</sup> others did not.<sup>11–13</sup> Most of these calculations were performed before a significant amount of low-energy  $\Lambda$ - $N$  scattering data<sup>14,15</sup> was available. In Ref. 6,  $\Lambda$ - $N$  potentials with hard cores were obtained which were reasonably consistent with the binding energies of the light hypernuclei and the low-energy  $\Lambda$ - $N$  scattering data. The importance of the hard core may be tested in a nonvariational way by investigating whether results for the hypertriton binding energy and the  $\Lambda$ - $N$  low-energy cross section consistent with experiment can be obtained from the three-body formalism and the simple “no core”  $\Lambda$ - $N$  potentials considered here.<sup>16</sup>

Our motivation for investigating the  $\Lambda$ - $d$  problem

when the work of A was in progress. At present the  $K^-$ - $N$  analysis is still on the basis of a zero-range model [see Jae Kwan Kim, Phys. Rev. Letters **14**, 29 (1965)] while the value for the low-energy  $K^+$ - $N$  isospin-zero amplitude is very uncertain [see V. J. Stenger, W. E. Slater, D. H. Stork, H. K. Ticho, G. Goldhaber, and S. Goldhaber, Phys. Rev. **134**, B1111 (1964)].

<sup>8</sup>  $\Lambda$ - $d$  scattering might also yield information on the off-energy-shell  $\Lambda$ - $N$  amplitudes once the on-shell amplitudes are more accurately known.

<sup>9</sup> K. Dietrich, H. J. Mang, and R. Folk, Nucl. Phys. **50**, 177 (1964) used an independent pair approximation and a self-consistent perturbation calculation.

<sup>10</sup> B. W. Downs, D. R. Smith, and T. N. Truong, Phys. Rev. **129**, 2730 (1963); D. R. Smith and D. W. Downs, *ibid.* **133**, B461 (1964); B. Ram and B. W. Downs, *ibid.* **133**, B420 (1964).

<sup>11</sup> R. H. Dalitz and B. W. Downs, Phys. Rev. **110**, 958 (1958).

<sup>12</sup> B. W. Downs and R. H. Dalitz, Phys. Rev. **114**, 593 (1959).

<sup>13</sup> G. Rajasekaran and S. N. Biswas, Phys. Rev. **122**, 712 (1961).

<sup>14</sup> B. Sechi-Zorn, R. A. Burstein, T. B. Day, B. Kehoe, and G. A. Snow, Phys. Rev. Letters **13**, 282 (1964).

<sup>15</sup> G. Alexander, U. Karshon, A. Shapira, G. Yekutieli, R. Englemann, H. Filthuth, A. Fridman, and A. Minguzzi-Ranzi, Phys. Rev. Letters **13**, 484 (1964).

<sup>16</sup> An analysis of the 3-body system,  $\Lambda$ + two nucleons, when the 2-body potentials contain a repulsive core is in progress.

\* Work supported by the U. S. Atomic Energy Commission.

† A preliminary report of this work was given at the January 1965 meeting of the APS in New York; Bull. Am. Phys. Soc. **10**, 19 (1965).

§ Present address: Department of Physics and Astronomy, Michigan State University, East Lansing, Michigan.

‡ Present address: Department of Physics, University of Southern California, Los Angeles, California.

<sup>1</sup> L. D. Faddeev, Zh. Eksperim. i Teor. Fiz. **39**, 1459 (1960) [English transl.: Soviet Phys.—JETP **12**, 1014 (1961)]; Dokl. Akad. Nauk SSSR **138**, 561 (1961); **145**, 301 (1962) [English transl.: Soviet Phys.—Doklady **6**, 384 (1961); **7**, 600 (1963)].

<sup>2</sup> Y. Yamaguchi, Phys. Rev. **95**, 1628 (1954).

<sup>3</sup> For similar work on the three-nucleon problem see R. Aaron, R. D. Amado, and Y. Y. Yam, Phys. Rev. Letters **13**, 574 (1964); and A. N. Mitra and V. S. Bhasin, Phys. Rev. **131**, 1625 (1963).

<sup>4</sup> J. H. Hetherington and L. H. Schick, Phys. Rev. **137**, B935 (1965). Hereafter referred to as A.

<sup>5</sup> J. H. Hetherington and L. H. Schick, Phys. Rev. **138**, B1411 (1965).

<sup>6</sup> See for example R. C. Herdon, Y. C. Tang, and E. W. Schmid, Phys. Rev. **137**, B924 (1965).

<sup>7</sup> The situation for the  $K^-$ - $N$  amplitudes is not as bad as it was

therefore is threefold. First, we wish to extend the three-body formalism previously developed to a case for which all the low-energy two-particle amplitudes are large and nonabsorptive. Second, we wish to determine if the low-energy  $\Lambda$ - $d$  cross sections are at all sensitive to the low-energy  $\Lambda$ - $N$  scattering parameters. Third, we wish to investigate the possibility of fitting both the low-energy  $\Lambda$ - $N$  scattering data and the hypertriton binding energy with a "no core"  $\Lambda$ - $N$  potential.

The details of the three-body formalism used here are almost identical to those used in A where a detailed discussion of this formalism may be found. A brief discussion of those parts of this formalism that are particular to the present work is given in the Appendix.

In the next section we give the form used for the two-body potentials. The values and their origins for the  $n$ - $p$  and  $\Lambda$ - $N$  potential parameters are also given.

In Sec. IIIA results for the binding energy of the hypertriton are presented for the sets of  $\Lambda$ - $N$  parameters discussed in Sec. II. Fits to the low-energy  $\Lambda$ - $N$  scattering data are given and discussed along with the  ${}^{\Lambda}\text{H}^3$  binding energy results.

In part B of Sec. III results for  $\Lambda$ - $d$  elastic and total cross sections for several of the sets of  $\Lambda$ - $N$  parameters discussed previously are presented. In these calculations the incident- $\Lambda$  lab momentum ranges from just above the threshold for deuteron breakup to 250 MeV/ $c$ . Both the doublet and quartet  $S$ -wave amplitudes are investigated in some detail over a wider momentum range.

The work is summarized in Sec. IV.

## II. TWO-BODY PARAMETERS

We let particle 2 be the  $\Lambda$  and particles 1 and 3 the nucleons. Of these three particles the  $\Lambda$  has isospin zero while the nucleons are treated as members of an isospin doublet coupled to form a state of zero isospin. The total isospin and the isospin of the pair of nucleons are constants of the motion.

Each of the three particles is a spin- $\frac{1}{2}$  fermion. The spin of the three-body system is either  $\frac{1}{2}$  (doublet state) or  $\frac{3}{2}$  (quartet state) and these states are orthogonal. The two-body potentials between pairs of particles are taken to be  $S$ -wave spin-dependent potentials. As the nucleons are identical we have a total of three two-body potentials; the  $N$ - $N$  potential in the  ${}^3S_1$  state, and the  $\Lambda$ - $V$   ${}^3S_1$  and  ${}^1S_0$  potentials.

Each two-body potential is taken to be an NLS potential. If  $V_i$  is the potential-energy operator between the  $i$ th pair of particles (i.e., between particles  $j$  and  $k$  with  $i \neq j$ ,  $i \neq k$ ,  $k \neq j$ ) then in terms of spin and configuration-space matrix elements

$$\langle \mathbf{r}_{jk}; s | V_i | \mathbf{r}_{jk}; s' \rangle = \lambda_i(s) v_i(\mathbf{r}_{jk}, s) v_i(\mathbf{r}_{jk}', s') \delta_{s, s'}, \quad (2.1)$$

where  $\mathbf{r}_{jk}$  is the relative position vector of particles  $j$  and  $k$ ,  $r_{jk} = |\mathbf{r}_{jk}|$  and  $s = s'$  is the total spin of this pair of particles. The potential shapes  $v_i(\mathbf{r}, s)$  are all taken

to have the form

$$v_i(\mathbf{r}, s) = (4\pi r)^{-1} \exp[-\beta_i(s)r]. \quad (2.2)$$

The parameters  $\lambda_i(s)$  and  $\beta_i(s)$  are determined from the relevant low-energy data. To aid in this determination we used the fact that for the potential given by the above equations the scattering length  $a_i(s)$  and effective range  $r_{0i}(s)$  are<sup>17</sup>

$$a_i(s) = \frac{2}{\beta_i(s)} \left[ 1 + \frac{4\pi\beta_i^3(s)}{\mu_i\lambda_i(s)} \right]^{-1}, \quad (2.3)$$

$$r_{0i}(s) = \frac{1}{\beta_i(s)} \left[ 1 - \frac{8\pi\beta_i^3(s)}{\mu_i\lambda_i(s)} \right], \quad (2.4)$$

where  $\mu_i$  is the reduced mass of particles  $j$  and  $k$ . Because of the identity of the nucleons it is possible to use the more convenient notation

$$a_0 = a_1(0) = a_3(0), \quad r_{00} = r_{01}(0) = r_{03}(0), \quad \dots, \quad (2.5)$$

$$a_1 = a_1(1) = a_3(1), \quad r_{01} = r_{01}(1) = r_{03}(1), \quad \dots, \quad (2.6)$$

$$a_2 = a_2(1), \quad r_{02} = r_{02}(1), \quad \lambda_2 = \lambda_2(1), \quad \dots. \quad (2.7)$$

For the nucleon-nucleon potential we have taken the values of the parameters that fit the low-energy data directly from Ref. 2. With  $B = 2.225$  MeV as the deuteron binding energy, these values are

$$\alpha_2 = (2\mu_2 B)^{1/2} = 45.706 \text{ MeV}/c, \quad (2.8)$$

$$\beta_2 = 6.255\alpha_2, \quad (2.9)$$

$$\lambda_2 = -4\pi\beta_2(\alpha_2 + \beta_2)^2/\mu_2. \quad (2.10)$$

There were three different sets of  $\Lambda$ - $N$  scattering lengths and effective ranges from which we chose our  $\Lambda$ - $N$  parameters.<sup>18</sup> These are shown in Table I. The first set was obtained by DeSwart and Dullemond<sup>19</sup> from the Dalitz and Downs<sup>12,20</sup> analysis of the light hypernuclei. It was assumed in this analysis that the  $\Lambda$ - $N$  potential was a purely attractive Yukawa potential with an intrinsic range of 1.5 F (corresponding to the

TABLE I. Scattering lengths and effective ranges for the  $\Lambda$ - $N$  interaction.

Set <sup>a</sup>	Singlet		Triplet	
	$a_0$ (F)	$r_{00}$ (F)	$a_1$ (F)	$r_{01}$ (F)
1	$-(2.4_{-0.6}^{+1.2})$	2	$-0.52 \pm 0.12$	4
2	$-(3.6_{-0.6}^{+3.6})$	2	$-0.53 \pm 0.12$	5
3	$-(2.89_{-0.41}^{+0.69})$	$1.94 \pm 0.08$	$-0.71 \pm 0.06$	$3.75 \pm 0.22$

<sup>a</sup> Sets 1 and 2 are taken from Ref. 19. Set 3 is from Ref. 6.

<sup>17</sup> We are using the convention for the scattering length  $k \cot \delta = -1/a + \dots$ .

<sup>18</sup> We have taken the  $\Lambda$ - $N$  singlet interaction to be more attractive than the triplet as is believed to be the case—see, for example, R. H. Dalitz, in *Proceedings of the Rutherford Jubilee International Conference* (Heywood and Company, Ltd., London, 1961), p. 103.

<sup>19</sup> J. J. de Swart and C. Dullemond, *Ann. Phys. (N. Y.)* **19**, 458 (1962).

<sup>20</sup> R. H. Dalitz and B. W. Downs, *Phys. Rev.* **111**, 967 (1958).

TABLE II. The effective ranges and corresponding range parameters for several values of the scattering lengths for Yukawa-shaped nonlocal separable  $\Lambda$ - $N$  potential.

Set	Singlet			Triplet		
	$a_0$ (F)	$r_{00}$ (F)	$\beta_0^{-1}$ (F)	$a_1$ (F)	$r_{01}$ (F)	$\beta_1^{-1}$ (F)
A	-2.0	2.0	0.500	-0.52	3.4	0.500
B	-2.4	1.92	0.500	-0.52	3.4	0.500
C	-2.4	1.92	0.500	-0.40	4.0	0.500
D	-1.8	2.06	0.500	-0.40	4.0	0.500
1	-2.4	2.0	0.518	-0.52	4.0	0.552
	-1.8	2.0	0.489	-0.40	4.0	0.500

exchange of two pions) in both the singlet and triplet spin states. DeSwart and Dullemond also gave (set 2 of Table I) the  $\Lambda$ - $N$  scattering lengths and effective ranges obtained by averaging together the results of Dalitz and Downs with those of Dietrich *et al.*<sup>9</sup> For each of their  $\Lambda$ - $N$  potentials this latter group used a hard core inside of a square well. The third set of parameters in Table I is taken from Ref. 6 where a hard core inside of an exponential well is the form used for each  $\Lambda$ - $N$  potential. We shall refer to the central values of sets 2 and 3 as sets 2c and 3c, respectively.

Our NLS  $\Lambda$ - $N$  potentials do not have a repulsive core. For consistency we chose to perform most of our calculations using parameters based on the first set of parameters given in Table I. Rather than use both the scattering length and effective range from this set, we used the scattering length—whose contribution to the two-body amplitude dominates that of the effective range in the energy range of interest—and the same intrinsic range as used by Dalitz and Downs.<sup>21</sup> For the NLS potential described above it is easily seen that if  $b \equiv b_0 = b_1$  is the intrinsic range for the singlet and triplet states, then with  $b = 1.5 F$

$$\beta^{-1} = \beta_0 = \beta_1 = \frac{1}{3}b = 0.5 F. \quad (2.11)$$

For several scattering lengths Table II compares the  $\Lambda$ - $N$  effective ranges and the quantities  $\beta^{-1}$  as determined in this manner with the original effective ranges and the  $\beta^{-1}$ 's determined by solving Eqs. (2.3) and (2.4). The differences do not seem to be significant.

### III. RESULTS

#### A. $\Lambda H^3$ Binding and $\Lambda$ - $N$ Scattering

In Table III we give the results of our calculation of  $B_\Lambda$  the binding energy of the  $\Lambda$  in the hypertriton.

TABLE III. Binding energy of the  $\Lambda$  in the hypertriton for several sets of  $\Lambda$ - $N$  parameters.\*

Set	A	B	C	D	2c	3c
$B_\Lambda$ (MeV)	0.20	0.48	0.37	0.05	1.01	0.90

\* The experimental value is taken to be  $B = 0.2$  MeV, but see Ref. 22.

<sup>21</sup> No such adjustments were made for sets 2 and 3 which, because they each contain the effects of a hard core, are already inconsistent with our model of the  $\Lambda$ - $N$  potential.

The experimental value for  $B_\Lambda$  was taken to be 0.2 MeV<sup>22</sup> and the hypertriton was taken<sup>18</sup> to have spin  $\frac{1}{2}$  as well as zero orbital angular momentum. With the  $\Lambda$ - $N$  ranges fixed at 0.5 F the values of the scattering lengths were varied by trial and error within the set I limits given in Table I until a set (set A of Table II) was obtained which gave the experimental value for  $B_\Lambda$ . Sets B, C, D are three of the sets used in this trial and error procedure. We list the values of  $B_\Lambda$  obtained for these sets to illustrate the sensitivity of the binding energy to the low-energy  $\Lambda$ - $N$  parameters. All of the sets A through D give values for  $B_\Lambda$  of about the right size<sup>22</sup>; i.e., no gross distortion has been introduced by switching from the local Yukawa  $\Lambda$ - $N$  potentials, used in Ref. 12, to the "equivalent" NLS potentials used here.

Sets 2c and 3c contain the effects of including a hard core; e.g., from Tables II and III we see that  $a_0$  is considerably larger for these sets than it is in any of sets A through D. In our model the  $\Lambda$ - $N$  potentials are purely attractive. As may be seen from the last two columns of Table III the result of fitting these purely attractive NLS potentials to low-energy parameters determined from potentials that include a hard core, is

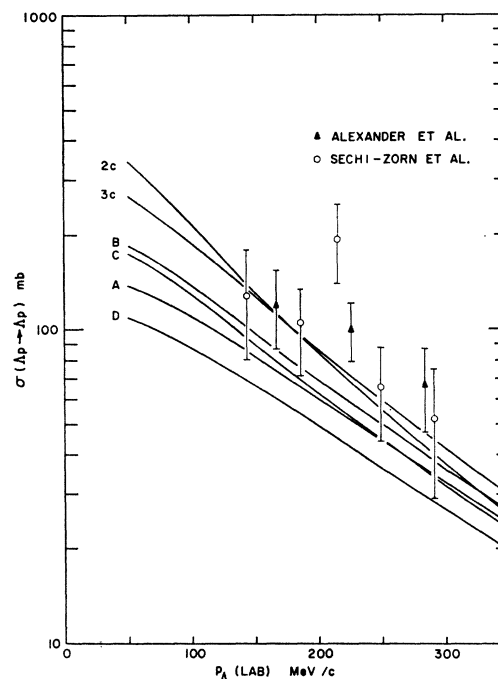


FIG. 1. Low-energy  $\Lambda$ - $p$  elastic-scattering cross sections derived from the nonlocal separable potential used in this paper fitted to six sets of  $\Lambda$ - $N$  parameters listed in Tables I and II. The experimental results are from Refs. 14 and 15.

<sup>22</sup> The experimental value of  $B_\Lambda$  is somewhat uncertain but seems to be in the region 0.0–0.4 MeV. The 3rd set of parameters in Table I is based upon  $B_\Lambda = 0.31 \pm 0.15$  MeV. See R. Levi-Setti, Proceedings of the International Conference on Hyperfragments, St. Cergue, Switzerland, 1963 (unpublished) for a summary of the binding energy data.

to make these NLS potentials far too attractive; i.e.,  $B_A$  is too large by about 0.7 MeV.

With regard to matching the low-energy  $\Lambda$ - $N$  scattering data however, the situation is reversed. In Fig. 1 we have plotted the low-energy  $\Lambda$ - $p$  elastic-scattering data<sup>14,15</sup> and the cross sections obtained from our NLS  $S$ -wave  $\Lambda$ - $N$  potentials fitted in turn to each of the sets 2c, 3c, A,  $\dots$ , D. Here sets 2c and 3c give a better fit to the data than sets A through D. The latter four sets are not attractive enough in the sense that each has an  $a_0$ —and hence a  $\Lambda$ - $N$  cross section—that is too small.<sup>23</sup> A consistent calculation with hard cores included should therefore give an  $a_0$  of the proper size to fit the  $\Lambda$ - $N$  cross section and give the correct value for  $B_A$  as well.

Each of the sets of  $\Lambda$ - $N$  parameters given in Table II was tested to see if any of them gave more than one bound state in the form of either a second doublet state, or a quartet state. None of them did.

**B.  $\Lambda$ - $d$  Scattering**

The results of our calculations of the  $\Lambda$ - $d$  scattering cross sections are presented in Figs. 2 through 6. All of these calculations except for one set of curves in Fig. 3 were performed using the set-A  $\Lambda$ - $N$  parameters.

In Fig. 2 we give the total and elastic  $\Lambda$ - $d$  cross sections for incident- $\Lambda$  lab momentum  $p_0$  in the range 100–250 MeV/ $c$ .<sup>24</sup> The cross sections for scattering in the quartet state ( $\sigma^Q$ ) and in the doublet state ( $\sigma^D$ ) individually as well as the average cross section ( $\sigma^A$ ), given by

$$\sigma^A = \frac{1}{3}\sigma^D + \frac{2}{3}\sigma^Q,$$

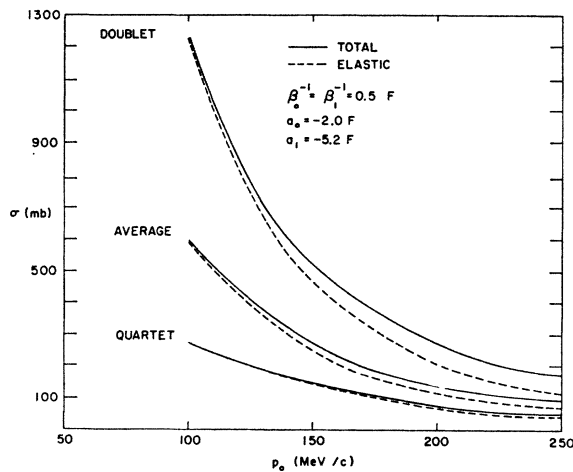


FIG. 2.  $\Lambda$ - $d$  elastic and total cross section for the set-A  $\Lambda$ - $N$  parameters. The doublet, quartet, and average cross sections are shown.

<sup>23</sup> The rather poor fit of all curves at the high end of the energy scale may reflect the need for the inclusion of a  $P$ -wave interaction at these energies.

<sup>24</sup> The threshold for deuteron breakup, i.e., inelastic scattering, is at  $p_0 = 88.95$  MeV/ $c$ .

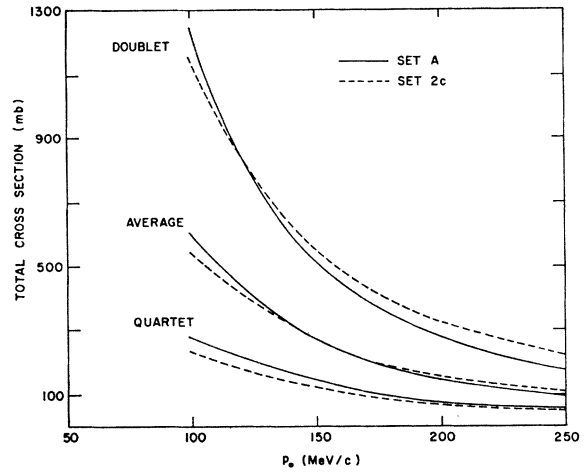


FIG. 3. The doublet, quartet, and average total  $\Lambda$ - $d$  cross sections for the A and 2c values of the  $\Lambda$ - $N$  parameters.

are presented. In Fig. 3 only the total cross sections are given but for both the set-A and the set-2c  $\Lambda$ - $N$  parameters. Clearly these cross sections are insensitive to the  $\Lambda$ - $N$  parameters in the energy region shown. At lower energies the effect on the doublet cross section of the 3-body bound state will become more pronounced. This cross section should then be quite different for sets of

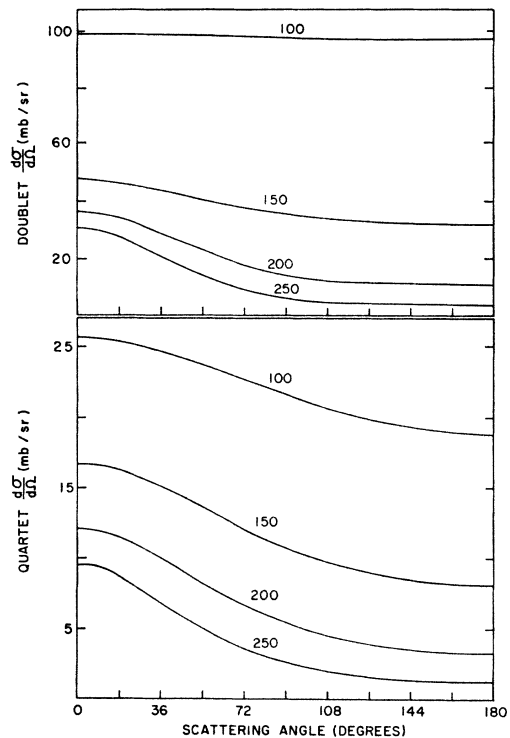


FIG. 4. Differential cross sections for  $\Lambda$ - $d$  quartet and doublet elastic scattering with the set-A values of the  $\Lambda$ - $N$  parameters. The curves are shown for  $\Lambda$  laboratory momenta  $p_0$  of 100, 150, 200, and 250 MeV/ $c$ . Note that the vertical scale is different in the upper and lower portions of the figure.

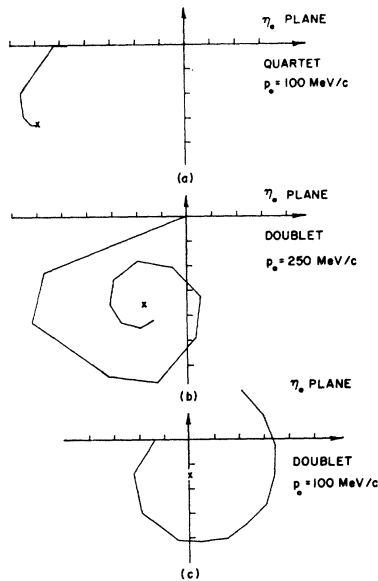


FIG. 5. Values of the  $S$ -wave scattering amplitude  $\eta_0$  for different orders of multiple scattering. (a) Quartet scattering at  $p_0=100$  MeV/ $c$ . (b) Doublet scattering at  $p_0=250$  MeV/ $c$ . (c) Doublet scattering at  $p_0=100$  MeV/ $c$ . The scale of (c) is reduced by a factor of 10 from that of (a) and (b). The cross in each diagram is the exact result. Set-A  $\Lambda$ - $N$  parameters are used throughout.

parameters such as  $A$  and  $2c$  that give such different values of  $B_\Lambda$ .<sup>25</sup> At higher energies than those shown in Figs. 2 and 3 the  $P$ -wave part of the 2-body amplitudes may become important.

Elastic angular distributions at  $p_0=100, 150, 200,$  and  $250$  MeV/ $c$  for both the doublet and quartet states are shown in Fig. 4. It is interesting that the angular distribution at  $p_0=100$  MeV/ $c$  is much flatter in the doublet state. The reason for this behavior is that at this energy the  $S$ -wave doublet bound state causes the  $S$ - and  $P$ -wave amplitudes in this state to be put about  $90^\circ$  out of phase; i.e., with  $\delta_0$  and  $\delta_1$  the  $S$ - and  $P$ -wave phase shifts, respectively, in the complex plane the vectors  $\exp(i\delta_0)\sin\delta_0$  and  $\exp(i\delta_1)\sin\delta_1$  are almost orthogonal. In the quartet state the phase difference between these amplitudes is small. This effect is also present in some degree at higher energies.

The last two figures in this section are presented to illustrate specifically the difference between the doublet and quartet  $S$ -wave brought about by the doublet  $S$ -wave bound state.

Figure 5 shows the various multiple-scattering (MS) contributions to the  $S$ -wave scattering amplitude  $\eta_0$  plotted in the complex  $\eta_0$  plane. In Fig. 5(a), where we have plotted the quartet amplitude at  $p_0=100$  MeV/ $c$ , the line segment with one end at the origin gives the contribution to  $\eta_0$  of the single scattering terms, the next segment is the contribution of the double scattering

<sup>25</sup> At low energies the dependence of the  $\Lambda$ - $d$  doublet cross section on the two-body scattering lengths is opposite to that of  $\Lambda$ - $N$  scattering, because the three-body cross section depends on its distance in the energy plane from the  $\Lambda H^3$  pole.

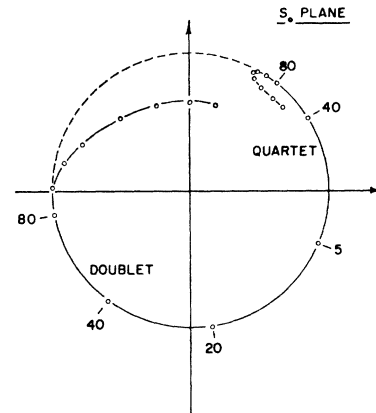


FIG. 6. Values of the  $l=0$  elastic  $\Lambda$ - $d$   $S$ -matrix elements for doublet and quartet scattering as functions of the  $\Lambda$  laboratory momentum  $p_0$ . The values of  $p_0$  shown are in MeV/ $c$ . In both curves the dots not labeled correspond to  $p_0=100, 125, 150, 200, 250, 300,$  and  $350$  MeV/ $c$ . The dashed curve represents the unit circle.

terms, and so on<sup>26</sup>; similarly, for Figs. 5(b) and 5(c) which give the  $S$ -wave doublet amplitude at  $p_0=250$  MeV/ $c$  and  $p_0=100$  MeV/ $c$ , respectively. The point  $\times$  in each diagram is the value of  $\eta_0$  when all MS terms are included; i.e., this is the value of  $\eta_0$  obtained when our set of MS integral equations is solved exactly by matrix inversion (see A) rather than iterated to give the contributions of the individual MS terms. The effect of the doublet bound state is clear. For the quartet state the MS series is rapidly convergent at  $p_0=100$  MeV/ $c$  (and therefore at higher energies also). For the doublet state the MS series converges only for values of  $p_0$  far enough away from the bound state. As may be seen from Figs. 5(b) and 5(c), the doublet MS series converges slowly at  $p_0=250$  MeV/ $c$  and not at all at  $p_0=100$  MeV/ $c$ .

We also calculated the  $S$ -wave  $S$ -matrix elements for both doublet and quartet scattering at values of  $p_0$  ranging from below the inelastic threshold to  $350$  MeV/ $c$ . The results are plotted in the  $S_0 = \exp(2i\delta_0)$  complex plane in Fig. 6. At a given value of  $p_0$  the (complex) value of  $S_0$  for the doublet (quartet) state is given by a point on the doublet (quartet) curve of this figure. For the doublet state  $S_0$  starts at  $+1$  ( $\delta_0=\pi$ ) for  $p_0=0$ , moves along the unit circle (the unitarity limit) clockwise as  $p_0$  increases, leaves this circle at the inelastic threshold, and continues moving within this circle with  $|S_0|$  decreasing as the inelastic scattering increases at higher  $p_0$ . There is no quartet bound state, so at  $p_0=0$ , although  $S_0=+1$ , as in the doublet case,  $\delta_0=0$ . The point representing  $S_0$  moves along the unit circle in a counterclockwise direction, leaves the unit circle at the inelastic threshold, and at a little higher value of  $p_0$  reverses directions; i.e.,  $\delta_0$  increases, becomes

<sup>26</sup> The single and doublet scattering terms are both real below the inelastic threshold ( $p_0=88.95$  MeV/ $c$ ). At  $p_0=100$  MeV/ $c$  the difference between the phase of each of these amplitudes and  $\pi$  was too small to show up in Fig. 5.

complex, and  $\text{Re}\delta_0$  goes through a maximum. The difference in the behavior of  $S_0$  as a function of  $p_0$  in the two cases is clearly distinguishable.

#### IV. SUMMARY

In this work we have assumed that the only potentials present in the isospin zero  $\Lambda+n+p$  system at low energies are the  $\Lambda$ - $N$   $^1S_0$  and  $^3S_1$  potentials and the  $N$ - $N$   $^3S_1$  potential. With NLS potentials for each of these we have solved the hypertriton binding energy problem and the low-energy  $\Lambda$ - $d$  scattering problem exactly.

We were not able to fit both the  ${}_\Lambda\text{H}^3$  binding energy and the low-energy  $\Lambda$ - $N$  scattering data with purely attractive  $\Lambda$ - $N$  potentials. We have presented some evidence to show this situation can be remedied if a hard core is included in each  $\Lambda$ - $N$  potential.

On the other hand, we have shown that for incident  $\Lambda$  lab momentum in the range 100–250 MeV/ $c$  the  $\Lambda$ - $d$  elastic and total cross sections are insensitive to the values of the  $\Lambda$ - $N$  potential parameters. We have presented both quartet and doublet angular distributions for one set of these parameters.

We have demonstrated explicitly that the presence of the doublet  $S$ -wave bound state causes the multiple scattering series for the scattering amplitude in this channel to diverge at low energy. Finally, we have described quantitatively the difference in the energy dependence of the  $S$ -wave doublet and quartet  $S$ -matrix elements caused by this bound state.

#### APPENDIX

It was shown in A that the determination of the  $l$ th partial-wave part of the elastic-scattering amplitude could be reduced to finding the solution to a set of coupled one-dimensional integral equations and averaging this solution over the  $l$ th partial-wave part of functions proportional to the initial and final states of the system. The development used here differs from that given in A only in the coupling together of the internal variables of the three particles. In A the two isospin- $\frac{1}{2}$  nucleons were coupled to form an isospin-zero state which in turn was coupled to the kaon to form a state with isospin  $\frac{1}{2}$ . Here the two spin- $\frac{1}{2}$  nucleons are coupled to form a spin-one state which is coupled to the  $\Lambda$  to form a state with spin  $\frac{1}{2}$  (doublet) or spin  $\frac{3}{2}$  (quartet).

We may represent the three two-body  $t$  matrices in the form of a diagonal matrix

$$[t_{\alpha\beta}] = \begin{bmatrix} t_1(0) & 0 & 0 \\ 0 & t_2(1) & 0 \\ 0 & 0 & t_1(1) \end{bmatrix},$$

where  $t_1(s)$  is the  $\Lambda$ - $N$   $t$  matrix in the spin state  $s$  and  $t_2(1)$  is the  ${}^3S_1$   $N$ - $N$   $t$  matrix. In this same space the kernel of our set of coupled integral equations is proportional to a matrix  $[W_{\alpha\beta}]$  of Racah coefficients, and the initial (and final) state of the system is proportional to a vector  $[C_\alpha]$ . Insofar as the spin space

coupling coefficients *only* are concerned, a typical term in the iteration of our solution for the scattering amplitude would have the form

$$\sum_{\alpha, \dots, \mu} C_\alpha t_{\alpha\beta} W_{\beta\gamma} \dots t_{\lambda\nu} W_{\nu\mu} C_\mu = \sum_{\alpha, \dots, \mu} C_\alpha t^\alpha W_{\alpha\gamma} \dots t^\lambda W_{\lambda\mu} C_\mu,$$

where  $[t^\alpha]$  is the “vector” whose elements are the diagonal terms of the matrix  $[t_{\alpha\beta}]$ .

In the  $\Lambda$ - $d$  problem we have

$$[W_{\alpha\beta}] = \begin{bmatrix} 1/2 & \sqrt{3/2} & -\sqrt{3/2} \\ \sqrt{3/2} & 0 & -1/\sqrt{2} \\ -\sqrt{3/2} & -1/\sqrt{2} & -1/2 \end{bmatrix},$$

with

$$[C_\alpha] = \begin{bmatrix} \sqrt{3/2} \\ 0 \\ -1/2 \end{bmatrix},$$

for the doublet state and

$$[W_{\alpha\beta}] = \begin{bmatrix} 0 & 0 & 0 \\ 0 & 0 & \sqrt{2} \\ 0 & \sqrt{2} & 1 \end{bmatrix},$$

with

$$[C_\alpha] = \begin{bmatrix} 0 \\ 0 \\ 1 \end{bmatrix},$$

for the quartet state.

The details of the numerics of the scattering calculation were about the same as they were in A.<sup>27</sup> We did find that above the threshold for deuteron breakup the large range (compared to the  $\bar{K}$ - $N$  range) of the  $\Lambda$ - $N$  potential allowed us to use a coarser mesh ( $72 \times 72$  points) than before in solving our set of integral equations. The functions in these equations are so rapidly varying below this threshold that even with a mesh of  $151 \times 151$  points we could do no better than obtain equality of the elastic and total cross sections to one part in  $10^3$ . As we approached zero energy (i.e., as our contour of integration ran closer to the singularity caused by the deuteron pole in the  $N$ - $N$   $t$  matrix) the behavior of these functions became so bad that even this accuracy could be obtained only with great difficulty.

The  ${}_\Lambda\text{H}^3$  binding-energy calculations were straightforward. We merely looked for a 3-body center-of-mass energy  $E_0$  for which the Fredholm determinant of our  $S$ -wave set of integral equations vanished; i.e., we looked for a pole in the  $l=0$  3-body  $t$  matrix. We searched for this zero of the Fredholm determinant by trial and error. It took of the order of 10 minutes of computer time to find  $B_\Lambda = |E_0| - 2.225$  MeV to within 0.01 MeV. In the energy region searched none of our contours of integration passed close by a singularity of the integrands, so that there were no difficulties with the numerics. A mesh size of  $117 \times 117$  points was sufficient to obtain the 0.01-MeV accuracy in  $B_\Lambda$ .

<sup>27</sup> All numerical work was performed on the CDC 1604 at the University of Minnesota Numerical Analysis Center.